

SIMULATION AND OPTIMIZATION OF A NEW ENERGY VEHICLE POWER BATTERY PACK STRUCTURE¹

GUANQIANG RUAN, CHANGQING YU, XING HU, JING HUA

School of Mechanical Engineering, Shanghai Dianji University, Shanghai, China
e-mail: hux@sdju.edu.cn

With the rapid growth in new energy vehicle industry, more and more new energy vehicle battery packs catch fire or even explode due to the internal short circuit. Comparing with traditional vehicles, the new energy vehicles industry should pay more attention to safety of power battery pack structures. The battery pack is an important barrier to protect the internal batteries. A battery pack structure model is imported into ANSYS for structural optimization under sharp acceleration, sharp turn and sharp deceleration turn conditions on the bumpy road. Based on the simulation, the battery pack structure is improved, and suitable materials are determined. Then the collision resistance of the optimized battery pack is verified, and the safety level is greatly improved. While ensuring the safety and reliability of the battery pack structure, it also reduces the weight to satisfy the lightweight design and complies with relevant technical standards.

Keywords: static, dynamic, modal, lightweight, optimization

1. Introduction

The energy crisis and environmental pollution have seriously affected economic development and people's living standards. New energy vehicles having huge advantages, such as low emissions and high energy saving, have been confirmed and widely approved by automobile manufacturers and governments. For new energy vehicles, the key component that affects vehicle safety is the battery pack. As the carrier of the battery, the importance of the battery pack cannot be underestimated. The strength, rigidity, heat dissipation and waterproof of the battery pack body should meet high design requirements (Feng and Hu, 2020).

When an electric vehicle crashes, slips out of control, or rolls over during driving, the power battery module would explode, short circuit, squeeze, leak, crack, and have displacement, which will cause mechanical damage, chemical damage, electrical damage, and combustion damage, and battery module explosion will lead to huge injuries to occupants in the electric vehicles (Du *et al.*, 2019; Aikhuele, 2020; Huang *et al.*, 2021). Therefore, when a car crashes during driving, the rigidity of the battery pack body must guarantee deformation of the battery element in its bearable range. Through the modeling and simulating of the battery pack of an electric car, the deformation and acceleration after loading are evaluated, which provides a reference for the optimal design of the battery pack structure.

This paper has established a numerical simulation model to study and optimize the structure of a new energy vehicle power battery pack. The model simulates statics and modal characteristics simultaneously and optimizes the structure at the same time, which not only meet the quality requirements, but also realize lightweight processing. Moreover, the model uses the natural vibration frequency of human organs as an evaluation standard during modal characteristics analysis, which could effectively improve the comfort of the human body.

¹Presented paper from the 4th International Conference on Material Strength and Applied Mechanics, MSAM 2021

2. Research status at home and abroad

2.1. Degree of research on the safety of new energy battery packs

In the history of research on automobile power battery packs, foreign countries have developed earlier and more mature than domestic ones. For example, Akbulut and Erol (2019) established a finite element model of the pack to investigate damped vibration characteristics of a prototype Li-ion battery pack, and it was observed that increasing the layer thickness led to a higher damping effect as expected. On the other hand, a monotonous augmentation of curing agent percentage did not result in a consistent rise or drop in the damping effect. Cicconi *et al.* (2020) proposed a modular approach to support the design of a battery pack considering Phase-Change Materials in the cooling system, and showed how a single module of cells could be stacked and how the cooling system of each module could be easily connected to each other. Greve *et al.* used radial compression, three-point bending and local indentation experimental methods to study the mechanical response characteristics of the battery, established a homogeneous battery model and accurately estimated the short-circuit inefficiency position of the battery under mechanical load, thereby obtained the easiest Damaged location and got improvement (Shi, 2011).

In China, Sun analyzed vibration and fatigue characteristics of a battery pack model, and made improvements in materials. Li Qiuming carried out static strength and modal tests of the battery pack box by materials, craft and CAE simulation, and optimized the analysis and conclusions. Chen Qi simulated random excitation on the model of the battery pack, tested fatigue performance, collected the road spectrum of the car, established a new kinematic model to predict the load of the battery pack, and analyzed and improved its fatigue performance by using the modal stress superposition method (Fan *et al.*, 2017).

2.2. Research status of structural optimization

In the 1960s, the Miceys applied the foundation structure method to topology optimization of discrete structures to confirm the load point and support point on the structure. In the 1980s, when Cheney studied the optimal structure of variable-thickness plates, he set the objective function as the maximum stiffness, got a variety of ribbed structures and found that the ribs can improve the structure, another one set the minimum flexibility as the objective function while optimizing the variable thickness, and set the corner base size of the finite element as the design variable, established the finite element method (Ma *et al.*, 2021). At the end of the last century, Kauai established an optimized genetic algorithm model, which is now used in material topology optimization design (Li *et al.*, 2021).

In China, Lin Yi *et al.* used the finite element method to optimize the topology of an automobile engine hood panel, and obtained the most suitable sheet metal structure and mechanical properties. In 2006, Gao, Meng *et al.* used CAE software to build an electric vehicle frame model, and optimized the topology of the model under static load bending and torsion conditions, and obtained the shape of the vehicle frame under multiple operating conditions (Zhang, 2011).

2.3. Comprehensive summary

Generally speaking, there are many unreasonable designs of the battery packs. The unreasonable structure will cause the stress to be greater than the yield stress of the material. Especially in a bumpy environment, resonance may occur under the influence of a certain vibration frequency, causing the internal short circuited, etc., which will affect the safety of the battery packs. In order to solve the above comprehensive difficulties, the key factor is to find the point with the greatest stress. Based on the optimization of the structure and the correct selection of battery

pack materials, the resonance could be avoided, and the durability of the battery pack could be improved. Many researches have been carried out on structural optimization at home and abroad, but there are very few studies on the optimization of the structure and modal coupling. Therefore, this article has conducted researches on the structure and modal coupling to fill up the deficiencies in this area.

3. Analysis and modeling of the battery pack structure

The computational and optimization process of the analyzed battery structure could be seen in Fig. 1.

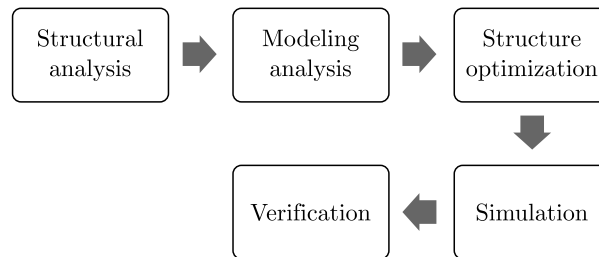


Fig. 1. Computational and optimization process

3.1. Structural analysis

The battery pack studied in this article is a lithium battery pack, which is located in the center of a car chassis. Its total power is 22 kWh, the battery capacity is 60 Ah, and the total voltage of the battery is 353 V. The battery element material is an aluminum structure made by ATL Pride with characteristics of large temperature difference withstand, higher peak value of electric heating, over 120 Wh/kg specific energy of the battery element, and 150-kilometers driving mileage. The battery pack is 1700 mm long, 1200 mm wide, and 210 mm high. The cover and the box are formed by stamping and die-casting aluminum steel, respectively. The entire box is fixed to the frame by 10 fixing bolts through connectors (Fig. 2a). Above, the weight of the entire box is about 235 kg. The main components of the battery pack have six parts. The outside is composed of the housing upper cover, the housing base and the lug connecting pieces. The upper cover and the base are connected by bolts, and the inside is composed of battery modules, fixing plates of battery modules and high liquid cooling plates, etc. The entire battery pack is fixed in the special groove with 10 bolts through the lug connection piece, and the groove is surrounded by the groove sheet on all sides. The finite element mesh model of the box can be seen in Fig. 2b.

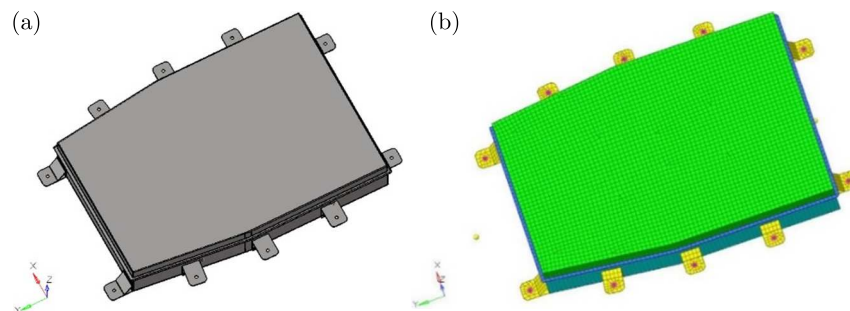


Fig. 2. (a) Geometric model of the battery pack, (b) finite element mesh model of the box

Table 1. Material properties of the aluminum alloy box

Material model	Elastic modulus [GPa]	Poisson's ratio	Density [kg/m ³]	Yield strength [MPa]
6061-T6	72	0.33	2800	276

3.2. Modeling analysis

In this paper, the modeling is carried out in accordance with the international standards of battery packs, and the static load shock and dynamic vibration of the battery packs under different working conditions are analyzed. The battery pack includes 8 modules, each module is composed of 12 battery elements, the module is fixed by bolts, the high-voltage connector connects the modules in series, and the box cover and box body are connected together by bolts. The input and output ports of the voltage interface and exhaust unit are installed on the surface of the battery pack.

First, a hyper mesh is imported. This software is compatible with most CAD formats, and can directly import the model before meshing. When dividing, it is necessary to strictly balance the size of the mesh and the ability of computer processing. Table 2 is the standard of mesh quality; all types of mesh division shall not exceed the standard range. According to the standard in the table, considering the size and structure of the battery pack and the accuracy required for simulation, it is decided to set the average mesh element size to 6 mm and design all elements of the battery pack as shell elements. Since the upper cover and the lower box occupy a larger surface area and are stressed more intensively, the 7 mm element mesh is used for division, and the 10 bolt-through holes are critical. As the stress is possibly concentrated, so the element mesh size is 2 mm, the mesh size of the remaining welded parts and the structure of the clap plate adhering to the side plate is 5 mm. The mesh shape can be triangle, quadrilateral or hexagon. Based on the above points of attention and the structural characteristics of the battery pack, the decision to divide the battery pack mesh is roughly listed: the total number of meshes of the battery pack is about 9815, and the number of nodes is 9,997. The control range of the mesh quality is that the minimum element size is 2 mm, the maximum element size is 10 mm, the mesh Jacobi ratio is 0.6, the warpage of all elements is below 15 degrees, the minimum angle of triangular elements is 31 degrees, and the maximum angle is 103 degrees. The number of triangular elements accounts for 7% of the total number of elements, and the maximum and minimum angles of quadrilateral elements are 120 degrees and 45 degrees, respectively.

Table 2. Mesh quality standards

Unit warpage	≤ 15	Maximum angle of triangle element	≤ 120
Unit twist angle	≤ 60	Minimum angle of triangle element	≥ 20
Jacobi ratio	≤ 0.7	Maximum angle of quadrilateral unit	≤ 135
Aspect ratio	≤ 5	Minimum angle of quadrilateral unit	≥ 45

3.3. Analysis of boundary conditions

In this paper, the battery pack is connected in series. Due to the complex internal structure of the module, the battery structure is simplified, and the weight of the battery cannot be ignored. Therefore, it is decided to use a mass point instead of the battery pack mass and apply 22 kg weight to each module. In order to make the simulation results more realistic, it was decided to impose corresponding constraints on the finite element model to imitate some constraints of the frame to the box, and stipulate that some directions of the structure should be blocked to prevent distortion of the simulation results. According to the special position and depth of the

battery pack simulation in the chassis groove, it is decided to apply four-sided constraints and upper and lower constraints simultaneously. The location of the constraint is also important, otherwise there may be stress concentration, so 36 bolts are added between the box cover and the box body, and six kinds of constraints are set, namely X , Y , Z three directions of movement constraints and rotation constraints around X , Y , Z , a two-layer constraint is adopted for each bolt.

The type of meshing at the connection is to set up rigid elements and retain a certain pre-tightening force to prevent an excessive bolt tightening force from affecting the performance of the material itself. A rigid unit is used instead of welding connection between the battery pack separator and the battery pack side plate, and the battery pack and the battery pack side plate are elastically connected by glue, so the box body and the module are connected by a one-dimensional elastic unit. The body and the box cover are fastened with two-dimensional rigid units to simulate bolts, and nonlinear contact is established between the battery pack and the box, and the box and the fastening bolts.

4. Static simulation of the battery pack

Static analysis refers to the internal stress analysis in which the entire battery pack system is not related to the applied load. The load deforms the side plate of the battery pack to achieve a stable effect. Its characteristic is that the stress and load imposed on the battery pack will not change with time.

When the battery pack is subjected to stress impact, its one unit three-dimensional model is respectively subjected to three different directions of stress. The strain effect per unit volume produced by these three stresses has been verified by multiple tests and is closer to the distortion energy density yield criterion, it is considered that the distortion energy density is the main basis for component deformation and damage (Liu *et al.*, 2019).

The density expression is

$$V_d = 1 + \frac{u}{6}E[(\sigma_y - \sigma_z)^2 + (\sigma_z - \sigma_x)^2 + (\sigma_x - \sigma_y)^2] \quad (4.1)$$

where σ_x , σ_y and σ_z are stresses along x , y and z , u is the displacement, and E means the elastic modulus.

Suppose the yield stress of the material is σ_s , and the distortion energy density is

$$V_d = 1 + \frac{u}{6}E(2\sigma_s^2) \quad (4.2)$$

The yield criterion of the material is

$$\sqrt{\frac{1}{2}[(\sigma_y - \sigma_z)^2 + (\sigma_z - \sigma_x)^2 + (\sigma_x - \sigma_y)^2]} \leq [\sigma] = \sigma_s \quad (4.3)$$

where $[\sigma]$ means the allowable stress.

On the macro side, it is necessary to start with the relationship between node displacement and node stiffness, and to introduce two mathematical expressions of the matrix and vector. Respectively denote the vector composed of all nodal displacements as \mathbf{P} , the vector composed of nodal loads as \mathbf{R} , and the structural stiffness matrix as \mathbf{K} , then the following relation is established (Mercuri *et al.*, 2020)

$$\mathbf{K}^*\mathbf{P} = \mathbf{R} \quad (4.4)$$

In this structural package, the material is aluminum, and the stiffness matrix \mathbf{K} is known. As long as a certain amount of load is applied, the displacement at each node can be known through (4.4), and then the force of each unit is calculated according to the correlation between the structural force and displacement.

4.1. Static strength working condition setting

When a car is driving on the road, it will inevitably encounter some potholes. The impact generated by these areas will be led to the frame by the tires, and then transmitted from the frame to the battery pack body. Thus it is very easy to cause longitudinal invisible damage or obvious deformation to the material and internal structure of the battery, while turning and acceleration and deceleration will cause stress on the transverse structure, which result in the material yield limit less than the maximum stress (Chung *et al.*, 2018). The following are three typical working conditions:

1. Bump and sharp turning conditions. This is to simulate the static state of the battery pack when the car turns at the intersection under bad road conditions. According to the literature and the actual state of the battery pack, it is decided to give the car a turning acceleration of 1 g, an acceleration of 1 g perpendicular to the ground when bumpy, and a gravity acceleration of 1 g.
2. Bumps and accelerated acceleration conditions. This is one of the most common conditions when vehicle driving. According to the literature, it is decided to give the car a 1 g acceleration in the forward direction, 1 g acceleration perpendicular to the road surface, and 1 g acceleration due to gravity.
3. Bump, acceleration, deceleration and turning conditions. When the car is decelerating rapidly, the car is accelerated by a 1 g in the opposite direction, when the centripetal acceleration is 1 g when turning, the acceleration perpendicular to the road surface is 1 g, and the gravity acceleration is 1 g.

4.2. Static analysis of the battery pack

Through the analysis and calculation of the finite element, under the acceleration load in all directions, the maximum load stress of the battery pack under ANSYS working condition 1 is 65.20 MPa, which is much lower than the yield limit of 6061-T6 material of 276 MPa (Fig. 3a). And the maximum stress occurs in the area where the lifting lug of the battery pack is connected with the box body, and the stress gradually decreases outward along the middle area. The calculated maximum displacement value is 83 mm, its position is in the middle of the upper cover and the deformation becomes smaller as it goes around (Fig. 3b). It can be explained that the battery module in the pack can absorb excess static deformation and displacement, and it can also ensure the battery core working normally, so the actual deformation will be much smaller, and it also has little influence on the internal high and low voltage wiring harness, basically in line with the battery pack static safety standards.

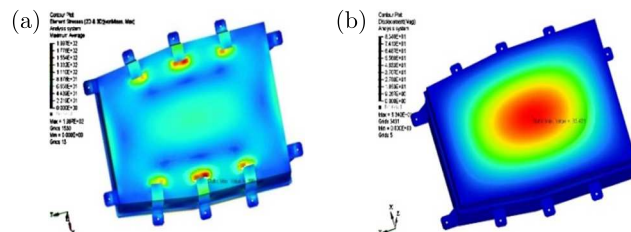


Fig. 3. (a) Stress and (b) displacement distribution of the battery pack body under working condition 1

When loading in working condition 2, a load is applied to the bottom of the box and the back side of the wall at 2 g and 1 g, respectively. The results in Fig. 4a show that the stress cloud map of the battery pack under this working condition is distributed on the upper surface, and the maximum stress is 203 MPa. The location is still between the contact point of the hanger and the box body, but it does not exceed the material yield stress of 276 MPa. The maximum

deformation is 86 mm, and located in the middle of the cover (Fig. 4b). After verification, it is concluded that the battery pack basically meets the safety performance requirements under this working condition.

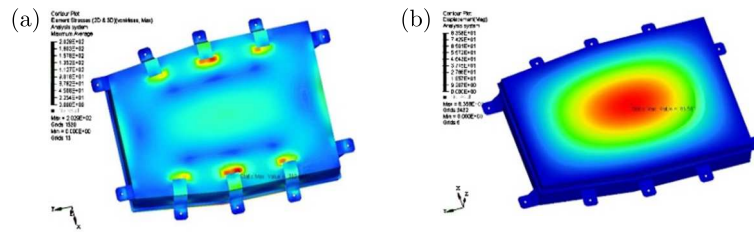


Fig. 4. (a) Stress and (b) displacement distribution of the battery pack body under working condition 2

Table 3. Static strength parameters

Working condition	x acceleration [g]	y acceleration [g]	z acceleration [g]
Bumpy and sharp turns	1	0	2
Bumpy and sharp acceleration	0	1	2
Bump acceleration and deceleration for turning	1	-1	2

Working condition 3 is a comprehensive performance condition which puts forward higher requirements on the material performance and position of each part of the box. The load as shown in Table 3 is simultaneously applied to the bottom, the front side and the right side of the box. The maximum stress of the battery pack is 204.2 MPa, and its location also acts on the connection between the hanging accessories and the box body to meet the yield strength of the aluminum alloy (Fig. 5a). The maximum variable value displayed is 83.7 mm, and its location is in the center of the upper cover (Fig. 5b). The calculation shows that it meets the safety standards under this working condition.

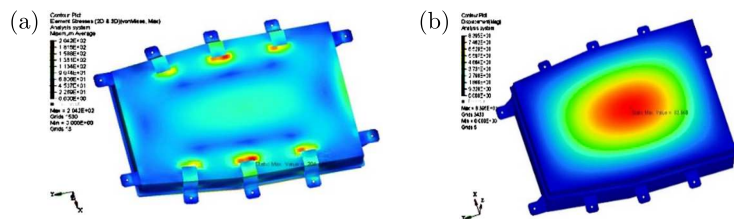


Fig. 5. (a) Stress and (b) displacement distribution of the battery pack body under working condition 3

5. Modal characteristics analysis of the battery pack

When the car is driving on a road, even if the material of the battery pack can overcome the continuous load impact brought by the outside in terms of static strength, it cannot fully guarantee that the battery pack shell will not be damaged by completely random external forces in different directions and sizes over time, or keep normal working for internal circuit components. After all, the car has a long time in driving and the working conditions are extremely complicated. The load change has exceeded the effect of static strength simulation, so taking dynamic analysis for the battery pack as a system in-depth, transforming the load into a function of time, can study the rationality and deficiencies of its internal structure more deeply, and carry out more comprehensive structural and material optimization.

The battery pack is set to be a free vibration mode, so the damping is very small and can be ignored (Tuononen and Lajunen, 2016). Considering the damping, the theoretical equation is

$$\mathbf{M}\ddot{\mathbf{u}}(t) + \mathbf{C}\dot{\mathbf{u}}(t) + \mathbf{K}\mathbf{u}(t) = \mathbf{P}(t) \quad (5.1)$$

where \mathbf{M} is the battery pack quality matrix, $\ddot{\mathbf{u}}(t)$ is the acceleration in global coordinates, \mathbf{C} is the battery pack damping matrix, $\dot{\mathbf{u}}(t)$ is the velocity in global coordinates, \mathbf{K} is the battery pack stiffness matrix, $\mathbf{u}(t)$ is the displacement in global coordinates, and $\mathbf{P}(t)$ is the total load vector.

Since it is free vibration, and $\mathbf{P}(t) = \mathbf{0}$, then the damping is ignored, hence

$$\mathbf{M}\ddot{\mathbf{u}}(t) + \mathbf{K}\mathbf{u}(t) = \mathbf{0} \quad (5.2)$$

The excitation of the battery pack vibration is simple harmonic motion, then set $\boldsymbol{\varphi}$ as the modal vector and ω as the natural frequency. According to equation (5.2), we could get

$$\mathbf{U} = \boldsymbol{\varphi} \sin(\omega t) \quad (5.3)$$

The characteristic equation and characteristic vector are

$$(\mathbf{K} - \mathbf{M}\omega^2)\boldsymbol{\varphi} = \mathbf{0} \quad (5.4)$$

Since the modal vector can not be zero, then

$$\mathbf{K} - \mathbf{M}\omega^2 = \mathbf{0} \quad (5.5)$$

Suppose the characteristic value is λ , from equation (5.5) we could get

$$\mathbf{K} - \mathbf{M}\lambda = \mathbf{0} \quad (5.6)$$

where \mathbf{M} and \mathbf{K} are orthogonal matrices of the order n , so

$$\begin{aligned} \boldsymbol{\varphi}_i^T \mathbf{M} \boldsymbol{\varphi}_j &= 0 & \boldsymbol{\varphi}_i^T \mathbf{K} \boldsymbol{\varphi}_j &= 0 & i &\neq j \\ \boldsymbol{\varphi}_j^T \mathbf{M} \boldsymbol{\varphi}_j &= m_j & \boldsymbol{\varphi}_j^T \mathbf{K} \boldsymbol{\varphi}_j &= k_j = m_j \omega^2 \end{aligned} \quad (5.7)$$

where k_j is the generalized stiffness and m_j is the generalized mass.

Since \mathbf{K} and \mathbf{M} are square matrices of the order n , equations (5.7) can be regarded as an equation with ω as an unknown number, and its order is n times. Finally, the natural frequencies of the battery pack satisfy

$$\omega_1 < \omega_2 < \omega_3 < \cdots < \omega_n \quad (5.8)$$

Each natural frequency corresponds to an amplitude $\boldsymbol{\varphi}$, and the quotient obtained by dividing adjacent amplitudes is the natural mode.

5.1. Modal analysis of the battery pack

There are many contents of dynamic response analysis, such as modal analysis, transient dynamic analysis, steady-state dynamic analysis, shock response analysis, random response analysis and buckling analysis. The modal analysis is the basis of the structural dynamic research. The correctness of the modal analysis directly affects the selection of battery pack materials and the improvement of structural lightweight, and also directly affects the correctness of the dynamic

response. Therefore, in all dynamic analysis, it is particularly important to simulate the correct modal conditions. It is the free mode and constrained mode mainly used to analyze the battery pack dynamically.

Modal analysis is used to study dynamic characteristics of a continuum structure. Each independent system has specific parameters such as mass, natural frequency, stiffness, damping and mode shape, and they are not affected by the external environment. However, each system has N modes, since the free vibration of the system is not restricted in any direction, which means its free vibration can be divided into N orthogonal single degree of freedom systems, each single degree of freedom system has a modal correspondence. According to the reference (Galos *et al.*, 2019), in the battery pack modal experiment, only the first seven natural modal vibration frequencies are required.

In addition to the processing of the excitation loading of the finite element model, the constraint method of the battery pack should be selected, which should be prepared in advance. As there are grooves around the box body to connect it, it is feasible to adjust the degree of freedom (DOF) of all bolts to 1 and constrain its box wall to reduce its DOF. The material of this model is defined as an aluminum alloy, type 6061-T6, and the density is defined as 2800 kg/m. Then, the assembly of each part is defined. In this battery pack, there are six bolts between the box cover and the lug, which are M6 bolts connected to the box cover and the lifting lug, and they are constrained by a smooth cylindrical hinge.

The battery pack is a separate physical object. According to the approximate frequency of the actual movement of the vehicle, the first ten-order vibration mode is used as a reference. The first-order vibration mode is particularly important, its natural frequency can be an important reference directly for the necessity to change the structure of the model, and to be the modal reference for the resonance of the vehicle body under external excitation.

5.2. Model simulation of the battery pack

The modal simulation is also carried out on the basis of processing of the finite element model. The goals are two, one is to check whether the battery structure has a bug or abnormal vibration caused by an unreasonable design, the other one is to see whether it overlaps with the natural frequency of the frame to avoid accidents caused by a long-term internal resonance of the battery, and also to improve the interior comfort. Based on the constrained modal analysis, the finite element model has been imported into the modal simulation in ANSYS to calculate the first ten-order natural frequencies. Since the battery is installed on the chassis, the box and the groove on the chassis are connected by bolts with lifting lugs, so the selected constrained mode will be closer to the real vibration environment of the battery pack than the free mode, the prerequisite condition of 6 degrees of freedom cannot be omitted in the modal link as shown in Figs. 6-10.

According to the results of modal simulation, the natural frequency of the first-order vibration mode is relatively low and may resonate with the frame. During the driving process of the vehicle, it is inevitable that there will be violent vibrations due to the unbalance of the wheels. When driving at high speed, the natural frequency of the frame is generally maintained at about 15 Hz. Based on the vibration requirements of high-speed driving, the first vibration mode of this battery pack is completely within the vibration frequency range of the frame, and the natural vibration frequency of the human organs is also between 5-15 Hz, so except for the first-order problem, the other vibration modes are basically within the safe frequency range which can be spotted in Table 4.

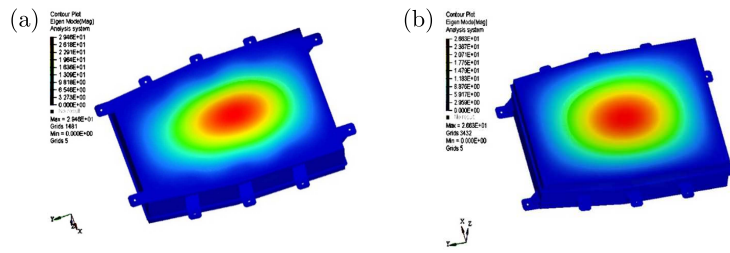


Fig. 6. (a) The 1st-order and (b) the 2nd-order mode of the battery pack

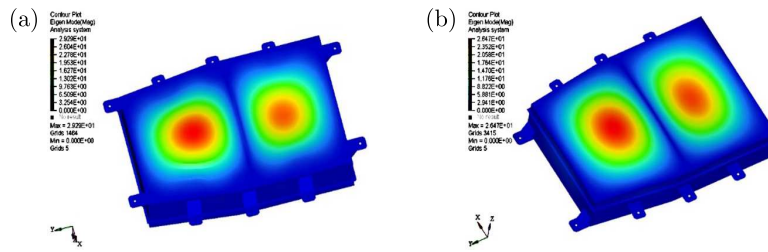


Fig. 7. (a) The 3rd-order and (b) the 4th-order mode of the battery pack

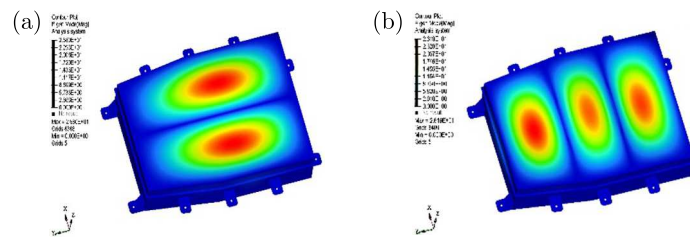


Fig. 8. (a) The 5th-order and (b) the 6th-order mode of the battery pack

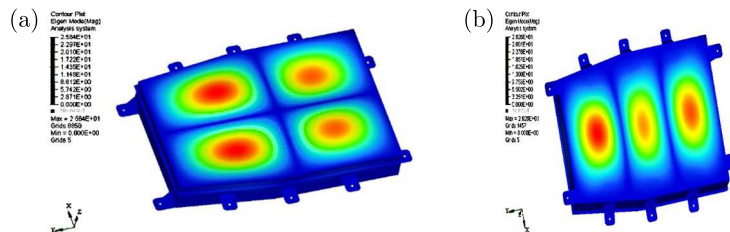


Fig. 9. (a) The 7th-order and (b) the 8th-order mode of the battery pack

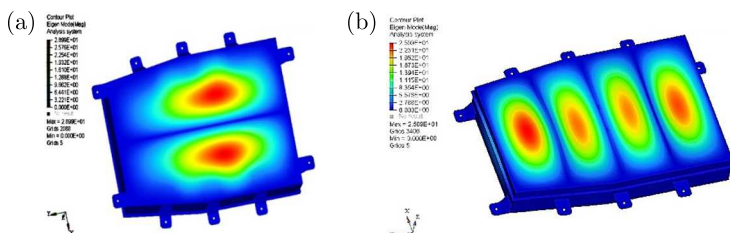


Fig. 10. (a) The 9th-order and (b) the 10th-order mode of the battery pack

Table 4. Constraint mode frequencies of each order of the battery pack

Order	Frequency [Hz]	Order	Frequency [Hz]
1	13.54	6	34.24
2	18.05	7	37.99
3	21.39	8	41.17
4	25.66	9	43.74
5	32.70	10	51.63

6. Optimization of the battery pack structure

In the previous Section, it had been explored that the potential locations of the battery pack structure may rupture the battery pack due to load and excitation vibration from the static and modal perspectives. The connection points between the lifting lugs and the box, and the middle of the top cover of the battery pack are the area most affected by the stress and the components with the largest deformation caused by the stress. In order to avoid the emergence of such dangerous parts, the lug connection and the upper cover should be optimized. In the static simulation, it was also found that the maximum stress was significantly smaller than the yield stress of the aluminum alloy material, so the distribution of the materials used was also considered in the optimization to ensure its lightweight. According to the repeated material distribution optimization and structural optimization demonstration on the ANSYS solver, it was found that adding a layer of reinforcing ribs which penetrates the lower case and cover of the battery pack can effectively improve the above shortcomings. The thickness of the reinforcing ribs is 4 mm, and the thickness of the original box is 2 mm, a total of 6 mm. In the process of static simulation, it was found that the stress on the surrounding sides was very small compared to the yield stress, and the box thickness range obtained by the solver was 1.2-1.8 mm. By making a trade-off between material saving and box rigidity, it is concluded that the optimal box thickness is reduced to 1.5 mm, while the safety against stress is also much better than before.

In the modal analysis, the natural frequency of the first-order vibration mode of the battery pack should effectively avoid the common frequency range under the normal driving state of the vehicle, and it is best to increase this frequency range by 5-10 Hz, so that the structure is in the safe range of vibration frequency.

6.1. Structural optimization verification

According to the above structural changes, the improvement of the optimized structural performance is analyzed again from the perspective of static stiffness and modal examination. First the static strength.

Working condition 1 is bumpy and sharp turning. The result shows that the maximum stress is 140.8 MPa after optimization, and its location is distributed near the edge line of the added rib and the box cover (Fig. 11a). The maximum deformation is 37.1 mm, which appears in the front, middle and rear of the box cover (Fig. 11b). Compared with the previous static simulation, the stress and maximum deformation are reduced by 30.09% and 54.59%, respectively.

Working condition 2 is bumpy and rapid acceleration. The maximum stress on the structure is 143.6 MPa, and its location is similar to the previous working condition (Fig. 12a). The maximum deformation is 38.2 mm, which is also distributed in the front and middle and rear positions of the box cover (Fig. 12b). Compared with the previous model, the maximum stress and the maximum deformation decreased by 29.2% and 54.3%, respectively.

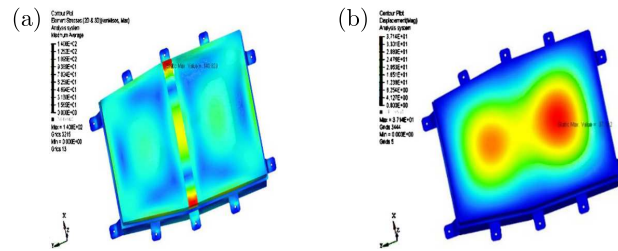


Fig. 11. (a) Stress and (b) strain of working condition 1 after optimization

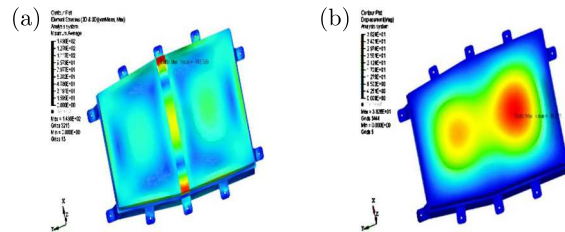


Fig. 12. (a) Stress and (b) strain of working condition 2 after optimization

Working condition 3 is bumpy, emergency braking and turning. According to the analysis, it is concluded that the maximum stress of the battery pack under this working condition is 142.6 MPa (Fig. 13a). Its location is still on the two sides where the ribs are in contact with the edge of the box cover. The maximum deformation in the middle rear position of the box is 40.0 mm (Fig. 13b). Compared with the original, the maximum stress and maximum deformation have been reduced by about 29% and 52%, respectively.

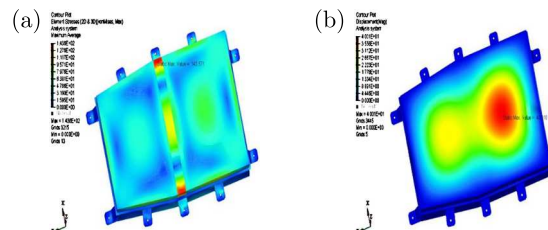


Fig. 13. (a) Stress and (b) strain of working condition 3 after optimization

Through optimization, the stress and deformation of each working condition are successfully reduced (Table 5). And the thickness of the battery pack body is reduced, the material is saved, and the overall weight of the battery goes down a lot. It is concluded that the optimized battery pack meets the use of security and structural reliability under these three load conditions.

6.2. Modal optimization verification

Modal optimization is mainly based on the 1st-order mode as an important reference. The structural optimization is mainly based on increasing the first-order natural frequency. By importing the optimized model into the ANSYS modal simulation solver, it is found that the maximum vibration frequency location of the first-order vibration mode of the optimized battery pack occurs at the rear of the upper cover instead of the center, as shown in Fig. 14. It is easier to control the shape change due to vibration. It is calculated that the first-order natural vibration frequency is 19.07 Hz, avoiding the high vibration frequency of about 15 Hz when the vehicle in motion, and to effectively avoid the possibility of box damage caused by resonance with the vehicle body effectively (Table 6).

Table 5. Comparison of optimization results under various working conditions

Working condition	Stress calculation result			Displacement calculation result		
	Before optimization [MPa]	Optimized [MPa]	Decrease percentage [%]	Before optimization [MPa]	Optimized [MPa]	Decrease percentage [%]
1	199.7	140.8	30.09	83.4	37.1	54.59
2	202.9	143.6	29.22	83.6	38.2	54.30
3	204.2	143.6	29.00	83.9	40.0	52.00

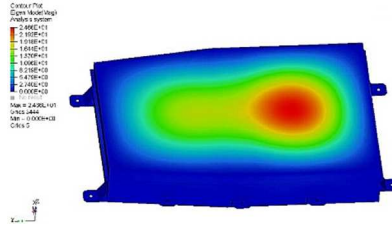


Fig. 14. The 1st-order mode of the battery pack after optimization

Table 6. Comparison of modal frequencies before and after optimization

Modal order	Before optimization [Hz]	After optimization [Hz]
1	13.54	19.07
2	18.05	21.98
3	21.39	23.92
4	25.66	28.41
5	32.70	35.04
6	34.24	37.61
7	37.99	39.74
8	41.17	45.63
9	43.74	51.05
10	51.63	55.48

7. Conclusion

In this paper, the battery pack of a new energy vehicle is studied, modeled and simulated by the finite element method. Hypermesh, ANSYS and other simulation analysis software are used to analyze the static strength and dynamic modal properties. Through finite element analysis and calculation, under acceleration loads in all directions, the maximum load stress of the battery pack under 1, 2 and 3 working conditions is 204.2 MPa. It is much lower than the yield limit of 6061-T6 material with a value of 276 MPa. And the maximum stress occurs in the connection area between the battery pack ears and the box. The maximum deformation is 86 mm, which is located in the middle of the lid. Therefore, the selection of the thickness is too conservative. According to the results of modal simulation, it can be seen that the natural frequency of the first-order mode is 13.54 Hz, and the natural frequencies of other modes are all greater than 15 Hz. The natural frequency of human organs is also between 5-15 Hz, so the natural frequency of all modes should be greater than 15 Hz as much as possible. These are common problems in the battery pack structures.

Then a simulation optimization model is established in the post-processing software. Finally, with the assistance of the Hypermesh solver, by adding reinforcing ribs, the battery toughness

is improved, the natural frequency is increased, and the amount of battery pack materials is reduced.

References

1. AIKHUELU D.O., 2020, Development of a fixable model for the reliability and safety evaluation of the components of a commercial lithium-ion battery, *Journal of Energy Storage*, **32**, 101819
2. AKBULUT M., EROL H., 2019, Damping layer application in design of robust battery pack for space equipment, *Applied Acoustics*, **150**, 81-88
3. CHUNG S.H., TANCOGNE-DEJEAN T., ZHU J., LUO H., WIERZBICKI T., 2018, Failure in lithium-ion batteries under transverse indentation loading, *Journal of Power Sources*, **389**, 148-159
4. CICONI P., KUMAR P., VARSHNEY P., 2020, A support approach for the modular design of Li-ion batteries: A test case with PCM, *Journal of Energy Storage*, **31**, 101684
5. DU J., LIU Y., MO X., LI Y., LI J., WU X., OUYANG M., 2019, Impact of high-power charging on the durability and safety of lithium batteries used in long-range battery electric vehicles, *Applied Energy*, **255**, 113793
6. FAN B., WANG F., LIU S., 2017, Development and application of drop test equipment for battery pack (in Chinese), *Chinese Journal of Power Sources*, **1**, 38-40
7. FENG X., HU J., 2020, Analysis and optimization control of finned heat dissipation performance for automobile power lithium battery pack, *Thermal Science*, **24**, 5B, 3405-3412
8. GALOS J., KHATIBI A.A., MOURITZ A.P., 2019, Vibration and acoustic properties of composites with embedded lithium-ion polymer batteries, *Composite Structures*, **220**, 677-686
9. HUANG W., FENG X., HAN X., ZHANG W., JIANG F., 2021, Questions and answers relating to lithium-ion battery safety issues, *Cell Reports Physical Science*, **2**, 1, 100285
10. LI H., XU B., LU G., DU C., HUANG N., 2021, Multi-objective optimization of PEM fuel cell by coupled significant variables recognition, surrogate models and a multi-objective genetic algorithm, *Energy Conversion and Management*, **236**, 114063
11. LIU B., GUO D., JIANG C., LI G., HUANG X., 2019, Stress optimization of smooth continuum structures based on the distortion strain energy density, *Computer Methods in Applied Mechanics and Engineering*, **343**, 276-296
12. MA X., XIONG K., YANG Q., WANG J., WANG L., 2021, A nonlinear shell augmented finite element method for geometrically nonlinear analysis of multiple fracture in thin laminated composites, *Thin-Walled Structures*, **161**, 107433
13. MERCURI V., BALDUZZI G., ASPRONE D., AURICCHIO F., 2020, Structural analysis of non-prismatic beams: Critical issues, accurate stress recovery, and analytical definition of the Finite Element (FE) stiffness matrix, *Engineering Structures*, **213**, 110252
14. SHI J., 2011, Electric vehicles and lightweight technology (in Chinese), *Automotive Technology and Materials*, **1**, 24-25
15. TUONONEN A., LAJUNEN A., 2016, Modal analysis of different drive train configurations in electric vehicles, *Journal of Vibration and Control*, **24**, 1, 126-136
16. ZHANG X., 2011, Thermal analysis of a cylindrical lithium-ion battery, *Electrochimica Acta*, **56**, 3, 1246-1255